

## Mapping quantum-well energy profiles of III-V heterostructures by scanning-tunneling-microscope-excited luminescence

Philippe Renaud and Santos F. Alvarado\*

*IBM Research Division, Zurich Research Laboratory, Säumerstrasse 4, 8803 Rüschlikon, Switzerland*

(Received 6 June 1991)

A technique has been developed that allows the energy profile of quantum wells in  $\text{Al}_x\text{Ga}_{1-x}\text{As}$  heterostructures to be mapped directly. The lateral resolution is a few nanometers, which allows the band-bending profile and the conduction-band discontinuity of interfaces within the heterostructure to be probed directly. The technique is based on the excitation of luminescence in the III-V compounds using the tip of a scanning tunneling microscope as a source of electrons.

Heterojunction devices consisting of epitaxial semiconductor layered structures have found wide application in microelectronics and solid-state devices. This has also promoted a tremendous growth in the field of semiconductor heterojunctions. The most important parameters to be controlled because they determine the electronic behavior of the heterostructure are the conduction- and valence-band-edge discontinuities<sup>1,2</sup> as well as the details of the band bending close to an interface. The development and characterization of semiconductor device structures require an even more detailed and accurate knowledge of their electronic and structural properties with nanometer resolution.

The invention of the scanning tunneling microscope (STM) (Ref. 3) inspired the development of characterization techniques with nanometer resolution. We report on a technique based on STM-induced luminescence that allows the conduction-band (CB) -edge discontinuity, band-bending profile, and depletion width at the interface to be measured directly with nanometer resolution.

For the present work we used Be-doped  $\text{Al}_x\text{Ga}_{1-x}\text{As}$  heterostructures with quantum wells formed by neighboring layers of different Al concentrations. The layers were grown by molecular-beam epitaxy along the [100] direction. The measurements were performed in ultrahigh vacuum conditions on (110) surfaces obtained by cleaving *in situ*. Under these conditions the STM produces cross-sectional images of the heterostructure. The STM tips were made of polycrystalline Ni.<sup>3</sup> The epitaxial structure is searched by recording the luminescence intensity while simultaneously recording the STM topographic image. The heterostructure is then easily identified in the luminescence image, where the bright stripes correspond to the wells.<sup>4</sup> Luminescence intensity spectra  $I_L$  versus  $V_T$  are acquired by sweeping  $V_T$  while the tunneling current  $i_T$  is kept constant by the feedback loop controlling the tunnel gap. Each spectrum represents an average of 4–10 curves. To obtain a profile of the CB across the heterostructure the tip is moved stepwise between each spectral measurement. The acquisition of each spectrum typically takes 30–60 s, while a scan across a heterostructure, which consists of 100–450 luminescence spectra, can take up to a few hours. For further experimental de-

tails see Refs. 4 and 5.

The STM-induced luminescence is described in a three-step model:<sup>5</sup> (i) vacuum tunneling from the tip to the surface of the semiconductor, (ii) transport of the electrons within the semiconductor, and (iii) radiative recombination. Consider the CB edge at the surface region of a *p*-type doped III-V compound exhibiting a downward band bending due to pinning of the Fermi level at the surface caused by contaminants or surface perturbations.<sup>4</sup> The STM tip emits electrons into the surface region via vacuum tunneling. At the surface the energy of these electrons in the CB is

$$\frac{\hbar^2 k^2}{2m^*} = \delta + V_T - E_C, \quad (1)$$

where  $V_T$  is the tip tunneling voltage,  $E_C$  is the CB energy, and  $\delta > 0$  is the downward band bending (see Fig. 1 inset). For  $eV_T > E_C$  a fraction of the injected electrons may ballistically cross the depletion region of width  $L_D$ , enter the bulk of the sample and, after radiative recombination, can be detected as a luminescence quantum of a characteristic photon energy. Radiative recombination occurs dominantly within the quantum wells due to the fact that the diffusion length of the thermalized electrons is much larger than the width of the thickest barriers (100 nm) in the multilayers used.<sup>4</sup> As can be seen in the inset of Fig. 1, tunneling is possible for  $eV_T > E_C - \delta$ , but electrons cannot be directly injected into the bulk unless  $eV_T > E_C$ , i.e., the threshold of luminescence due to recombination behind the depletion region is given by  $eV_T = E_C$ .

Figure 1 shows typical luminescence spectra acquired on an  $\text{Al}_{0.1}\text{Ga}_{0.9}\text{As}/\text{Al}_{0.3}\text{Ga}_{0.7}\text{As}$  heterojunction with a nominal Be-dopant concentration of  $p = 10^{19} \text{ cm}^{-3}$ . The threshold, determined by linear extrapolation in  $\sqrt{I_L}$  versus  $V_T$  plots of the data, appears at the expected energy. The quadratic response can be justified by extending the theoretical arguments used for injection of electrons from a metal into a semiconductor in a ballistic electron emission microscope<sup>6</sup> (BEEM) or for the case of internal photoemission,<sup>7</sup> where Fowler's law may be applicable. The basic assumptions are the conservation of energy and

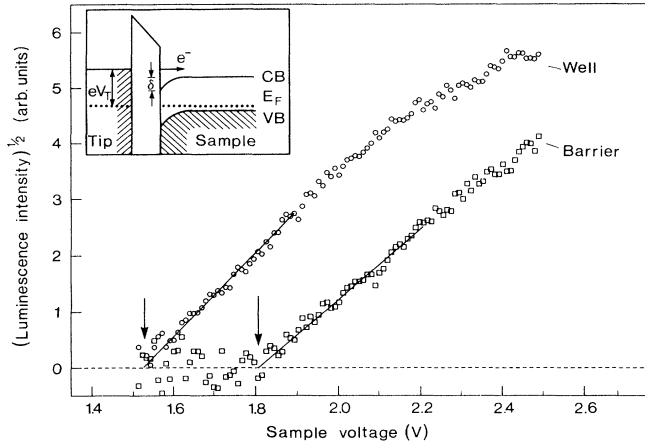


FIG. 1.  $(\text{Luminescence})^{1/2}$  vs voltage spectra on an  $\text{Al}_{0.1}\text{Ga}_{0.9}\text{As}/\text{Al}_{0.3}\text{Ga}_{0.7}\text{As}$  heterostructure. The upper spectrum was taken at a 100-nm well, and the lower spectrum was taken at a 50-nm barrier, both 20 nm away from the interface. The inset shows schematically the energy diagram of the tunneling junction and the semiconductor surface interface. VB and CB are the edges of the valence of the conduction bands, respectively, and  $E_F$  is the Fermi energy.

momentum parallel to the surface. As a result electrons may only cross the depletion region and reach the bulk if they are emitted from the surface region within an injection cone of half-width angle given by

$$\sin^2\Theta_c = \frac{m^*(eV_T - E_C)}{m^*(\delta + eV_T - E_C)} \frac{eV_T - E_C}{\delta + eV_T - E_C}, \quad (2)$$

where  $m^*(E)$  is the energy-dependent electron effective mass.<sup>8</sup> This is similar to the expression used in BEEM,<sup>6</sup> except that there the mass ratio  $m^*/m$  is taken,  $m$  being the free-electron mass. Ballistic electrons moving outside of the injection cone are reflected and trapped within the depletion region and may not contribute to the luminescence signal—the exceptions will be discussed below. Equation (2) shows that the injection cone becomes more acute for decreasing injection energy. This accounts for high spatial resolution in BEEM images.<sup>6</sup>

We note that Eq. (2) represents an upper limit of the injection cone and does not account for any electron impulse selection at the tunneling junction.<sup>9</sup> Equation (2) also shows that it is possible to determine the local electronic properties of interfaces with nanometer resolution. For the depletion region, however, the electron potential increases smoothly and hence the electron trajectories are not straight lines but curved such that the injection cone is transformed into an injection “trumpet” whose mouth angle decreases with decreasing injection energy. Still, high resolution can be achieved because only electrons within the center of the injection trumpet, i.e., those with small  $k_{\parallel}$ , experience less damping due to their shorter, almost straight, trajectory paths. Another implication of the smooth depletion region potential barrier is that quantum-mechanical reflection (QMR) effects may not be

dominant. QMR, important in sharp step potentials, may give rise to an  $I \propto V^{5/2}$  power law.<sup>10</sup> The present data do not allow us to determine exactly which power law fits best, but we do note that Fowler’s law provides a reasonably good fit and that the threshold determined by the extrapolation agrees very well with the expected CB edge, see Fig. 2. We also find that the extrapolated threshold decreases with increasing power-law strength. According to Ref. 10 the  $\frac{5}{2}$  power law would yield a threshold consistently 40–80 meV lower than that of Fowler’s law. Such a shift does not improve the agreement of our data with the band-edge position. It is important to note that we have found cases where the spectra collected at the wells do not fit Fowler’s law well but perhaps fits a weaker power law better. Such cases are characterized by a lower threshold (up to about 100 meV) than the expected bulk CB edge value and by a luminescence yield higher than in the Fowler regime. We attribute this observation to radiative surface recombination of electrons when the surface band bending is small,  $\delta \lesssim 100$  meV, such that the density of holes in the valence band is still high enough to allow a surface luminescence signal detectable with our apparatus. The open circles in Fig. 2 illustrate the occurrence of this effect. The magnitude of  $\delta$  depends on the concentration of surface adsorbates and/or defects. Hence we have been able to observe the quenching of surface luminescence caused by the cumulation of surface contaminants with time. For large band bending the Fermi level lies so far above the surface valence band that indirect or nonradiative recombination processes dominate over the direct radiative recombination rate which then drops below our appara-

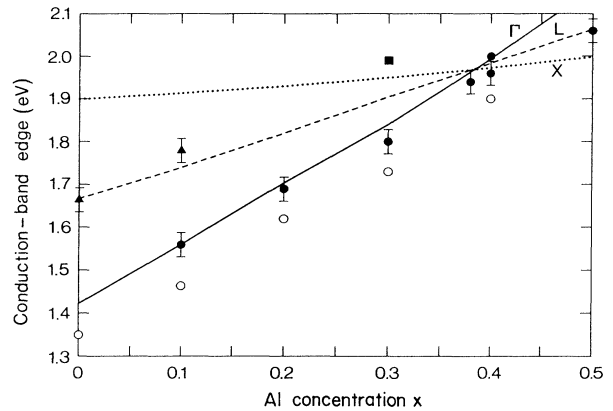


FIG. 2. Position of the conduction band determined from  $I_L$  vs  $V_T$  spectra on  $\text{Al}_x\text{Ga}_{1-x}\text{As}$  doped with  $p = 10^{19} \text{ cm}^{-3}$  Be. The solid circles represent the bulk band edge. The error bars indicate the scatter from measurements performed on different samples. The solid line is the conduction-band-edge energy, equal to the band gap (Ref. 11) when  $\text{VB} = E_F$ , which is approximately the situation for the heavy  $p$ -type doping level of the samples. The triangles and square show features which could be related to the injection of electrons into the  $L$  and  $X$  bands, represented by the dashed and dotted lines. The open circles are measured when radiative recombination at the surface is strong.

tive detection limit. Under such conditions the arguments leading to Eq. (2) may be applied and thus Fowler's law can be considered to be a good approximation to describe the  $I_L$  versus  $V_T$  spectra near threshold, which then corresponds to the bulk CB edge.

Figure 3 shows the CB profile measured from the luminescence threshold on a GaAs/Al<sub>0.38</sub>Ga<sub>0.62</sub>As multiple-quantum-well structure, Be-doped  $p = 10^{18}$  cm<sup>-3</sup>. This structure consists of a series of barrier/well pairs of 20, 10, 5, and 2 nm, respectively. To the right of the multiple-quantum-well structure we placed an Al<sub>0.38</sub>Ga<sub>0.62</sub>As barrier doped with  $p = 3 \times 10^{18}$  cm<sup>-3</sup> Be. The distance between each point is 1.5 nm. Measurements performed with a step size of 0.7 nm shows that the potential wall at the interface is confined to within 3–3.5 lattice unit cells (1.7–2.0 nm).<sup>12</sup> The solid line represents the expected position of the *bulk* CB edge energy as calculated by means of the heterostructure modeling program HETMOD using the nominal dimensions, composition and doping level of the heterostructure.<sup>13</sup> For the present structure the ground-state energy  $E_0$  is 230, 100, and 40 meV for the 2-, 5-, and 10-nm quantum wells, respectively. These levels have been indicated in Fig. 3. It can be seen that the measured luminescence threshold shows a clear tendency to increase when the size of the well decreases, in accordance with the quantum-well behavior described above. An accurate determination of these levels, however, becomes somewhat unreliable when the width of the quantum wells is comparable to the interface broadening observed with this technique.

The band bending and width of the depletion region measured on the Al<sub>0.38</sub>Ga<sub>0.62</sub>As barrier at the edge of the 100-nm well agrees with the calculated profile, see the right-hand part of the profile in Fig. 3. Furthermore a direct determination of the CB discontinuity  $\Delta E_{CB}$  at the interface is possible from the threshold profile.  $\Delta E_{CB}$  manifests itself as an abrupt change of the threshold at the interface, occurring typically within about 3.5 lattice units. After this sharp feature, going into the barrier, its edges appear rounded or, as for the 20-nm barrier, asymmetric. The asymmetry of the potential barrier could be due to different values of  $\Delta E_{CB}$  associated with the fact that the normal and inverted interfaces are not identical to uncontrolled interfacial adsorbates or to local fluctuations of the Al concentration.<sup>14</sup> For this particular case, however, we cannot completely rule out the occurrence of local spots where surface luminescence occurs, giving rise to lower thresholds. The best accuracy of the measurement of  $\Delta E_{CB}$  is given by the accuracy of the threshold determination, which for the present data can be about 20–30-meV rms. Measurements of  $\Delta E_{CB}$  performed on interfaces between various well/barrier com-

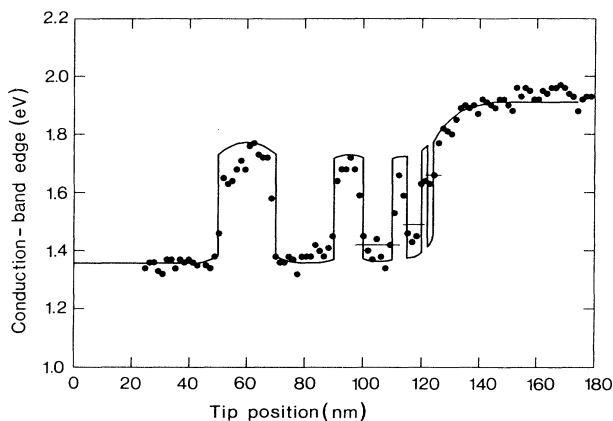


FIG. 3. Conduction-band profile measured by luminescence threshold on a GaAs/Al<sub>0.38</sub>Ga<sub>0.62</sub>As multiple-quantum-well structure. The wells are 20, 10, 5, and 2 nm wide with a Be doping level of  $p = 10^{18}$  cm<sup>-3</sup>. To the right of the quantum wells is a 100-nm barrier with  $p = 3 \times 10^{18}$  cm<sup>-3</sup>. The solid line is the calculated conduction-band edge. The horizontal lines across the quantum wells show the ground-state electronic level  $E_0$ .

binations yield results close, but not exactly equal, to the  $\Delta E_{CB} = \frac{2}{3} E_g$  rule, and are in reasonably good agreement with the HETMOD calculations. Note also that the height of the narrow barriers is only slightly higher than  $\Delta E_{CB}$  due to proximity effects. However when the barrier is more than twice as thick as the depletion width, the barrier height equals the band-gap difference between the two compounds.

We have demonstrated the possibility of performing *local* luminescence spectroscopy using the tip of a scanning tunneling microscope to inject electrons into Al<sub>x</sub>Ga<sub>1-x</sub>As heterostructures. This technique provides a *direct* measurement of the profile of the conduction-band minimum across the complex multilayer, thus allowing the following crucial interface parameters to be determined directly: conduction-band discontinuity, band bending, and width of the depletion region, as well as the energy of the quantized levels within single quantum well.

We are very thankful to H. P. Meier and D. J. Arent for providing the MBE heterostructures used in these experiments and to A. C. Warren for providing the heterostructure modeling program. Many thanks also to L. Perriard for lapping and to M. Richard for his continuous help in preparing the heterostructures for cleavage. We gratefully acknowledge fruitful conversations with H. Rohrer and C. K. Shih.

\*Electronic address: alv @ zurlvm1.

<sup>1</sup>*Heterostructures and Band Discontinuities*, edited by F. Capasso and G. Margaritondo (North-Holland, Amsterdam, 1987).

<sup>2</sup>J. Mendez, A. Pinczuk, D. J. Werder, A. C. Gossard, and J. H.

English, Phys. Rev. B **33**, 8863 (1986).

<sup>3</sup>G. Binnig, Ch. Gerber, E. Weibel, and H. Rohrer, Phys. Rev. Lett. **50**, 120 (1983).

<sup>4</sup>D. L. Abraham, A. Veider, Ch. Schönberg, H. P. Meier, D.

- J. Arent, and S. F. Alvarado, *Appl. Phys. Lett.* **56**, 1564 (1990).
- <sup>5</sup>S. F. Alvarado, Ph. Renaud, D. L. Abraham, Ch. Schönenberg, D. J. Arent, and H. P. Meier, *J. Vac. Sci. Technol. B* **9**, 409 (1991).
- <sup>6</sup>W. J. Kaiser and L. D. Bell, *Phys. Rev. Lett.* **60**, 1406 (1988); L. D. Bell and W. J. Kaiser, *ibid.* **61**, 2368 (1988).
- <sup>7</sup>J. S. Helmann and F. Sanchez-Sinencio, *Phys. Rev. B* **7**, 3702 (1973).
- <sup>8</sup>U. Rössler, *Solid State Commun.* **49**, 943 (1984).
- <sup>9</sup>H. De Raedt, N. Garcia, and J. J. Sáenz, *Phys. Rev. Lett.* **63**, 2260 (1989).
- <sup>10</sup>M. Prietsch and R. Ludecke, *Phys. Rev. Lett.* **66**, 2511 (1991).
- <sup>11</sup>See, for instance, M. Guzi and J. L. Staehli, *Solid State Phenomena* **10**, 25 (1989).
- <sup>12</sup>The transtion at the interface of a III-V heterostructure, as seen by STM, takes place within 1–2 unit cells, see, O. Albrektsen, D. J. Arent, H. P. Meier, and H. W. M. Selemink, *Apply. Phys. Lett.* **57**, 31 (1990); H. Salemink and O. Albrektsen, *J. Vac. Sci. Technol. B* **9**, 779 (1991).
- <sup>13</sup>R. A. Kiel, M. A. Olson, K. Yoh, S. L. Wright, M. Heiblum, J. Yates, and A. C. Warren, *Tech. Dig.—Int. Electron Devices Meet.* **1988**, 684.
- <sup>14</sup>*Electronic Structure of Semiconductor Heterojunctions*, edited by G. Margaritondo (Kluwer Academic, Dordrecht, 1988).